

**Derivation of Apollo 14 high-Al basalts at discrete times: Rb-Sr isotopic constraints.** Hejiu Hui<sup>1</sup>, Clive R. Neal<sup>1</sup>, Chi-Yu Shih<sup>2</sup> and Laurence E. Nyquist<sup>3</sup> <sup>1</sup>Department of Civil Engineering and Geological Sciences, University of Notre Dame, Notre Dame, IN 46556, <sup>2</sup>Jacobs Technology, ESCG, Mail Code JE23, Houston, TX 77058, <sup>3</sup>ARES, NASA-Johnson Space Center, Mail Code KR, Houston, TX 77058.

**Introduction:** Pristine Apollo 14 (A-14) high-Al basalts represent the oldest volcanic deposits returned from the Moon [1,2] and are relatively enriched in  $\text{Al}_2\text{O}_3$  (>11 wt%) compared to other mare basalts (7-11 wt%). Literature Rb-Sr isotopic data suggest there are at least three different eruption episodes for the A-14 high-Al basalts spanning the age range ~4.3 Ga to ~3.95 Ga [1,3]. Therefore, the high-Al basalts may record lunar mantle evolution between the formation of lunar crust (~4.4 Ga) and the main basin-filling mare volcanism (<3.85 Ga) [4]. The high-Al basalts were originally classified into five compositional groups [5,6], and then regrouped into three with a possible fourth comprising 14072 based on the whole-rock incompatible trace element (ITE) ratios and Rb-Sr radiometric ages [7]. However, Rb-Sr ages of these basalts from different laboratories may not be consistent with each other because of the use of different  $^{87}\text{Rb}$  decay constants [8] and different isochron derivation methods over the last four decades.

This study involved a literature search for Rb-Sr isotopic data previously reported for the high-Al basalts. With the re-calculated Rb-Sr radiometric ages, eruption episodes of A-14 high-Al basalts were determined, and their petrogenesis was investigated in light of the “new” Rb-Sr isotopic data and published trace element abundances of these basalts.

**Rb-Sr Isotopic Provenance:** The Rb-Sr isotopic data in the literature for pristine A-14 high-Al basalts [1,3, 10-21] were re-processed using the program *Isoplot 3.70* [9] with  $\lambda(^{87}\text{Rb}) = 0.01402 \text{ Ga}^{-1}$  [8].

**High-Al Basalt Eruption Episodes.** A plot of all re-calculated radiometric ages and initial  $^{87}\text{Sr}/^{86}\text{Sr}$  ( $I_{\text{Sr}}$ ) of A-14 high-Al basalts is not discriminatory in distinguishing the isotopic provenance of each group due to large  $2\sigma$  uncertainties associated with the calculated Rb-Sr ages and  $I_{\text{Sr}}$  (Fig. 1). Hence a weighted average age of each basalt group was calculated using the program *Isoplot 3.70* [9] (Fig. 1a). In the error-weighted average calculation, only errors from the isochron regression were propagated as  $2\sigma$  internal errors [9]. A weighted average of  $I_{\text{Sr}}$  for each basalt group was also calculated using the same method (Fig. 1b). The weighted average age represents the crystallization age of each high-Al basalt group (i.e., the magma eruption time).

This re-evaluation of the Rb-Sr isotopic age data shows that Group B basalts erupted at  $4.03 \pm 0.03 \text{ Ga}$  and after Group A basalts ( $4.24 \pm 0.10 \text{ Ga}$ ) but before Group C basalts ( $3.92 \pm 0.03 \text{ Ga}$ ) (Fig. 1a). Clast 14321,371 has similar age and  $I_{\text{Sr}}$  to basalt 14072 (Fig. 1) though no whole-rock trace element data are available to verify its group assignment. Therefore, we tentatively group it with 14072 to form Group D high-Al basalts. The weighted average crystallization age of Group D basalts is  $3.96 \pm 0.11 \text{ Ga}$ , which is indistinguishable from the ages of those from Groups B and C (Fig. 1a), partially due to the relatively large error. However, Group D basalts can be separated from Group A, B and C basalts in terms of weighted average of  $I_{\text{Sr}}$  (Fig. 1b). This indicates that Group D basalts derived from a different source region compared to Group B and C basalts, which is consistent with their ITE data [7, 22]. A plot of weighted average age versus weighted average  $I_{\text{Sr}}$  does distinguish the isotopic provenance of Group A, B and C basalts (Fig. 2).

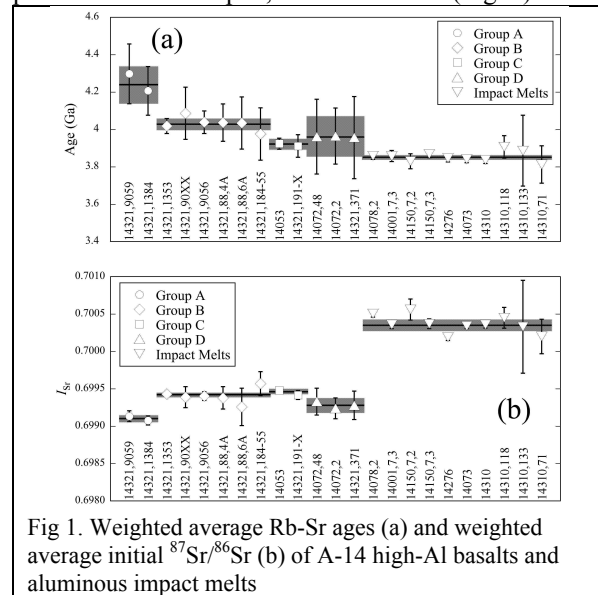


Fig 1. Weighted average Rb-Sr ages (a) and weighted average initial  $^{87}\text{Sr}/^{86}\text{Sr}$  (b) of A-14 high-Al basalts and aluminous impact melts

**Aluminous impact melts: Post-eruption activity.** A-14 aluminous impact melts have higher  $I_{\text{Sr}}$  and are younger than the pristine high-Al basalts (Fig. 1). They also contain distinctly different ITE abundances (KREEP-like) compared to high-Al basalts [7,22]. The weighted average age and  $I_{\text{Sr}}$  of A-14 aluminous impact melts are  $3.85 \pm 0.01 \text{ Ga}$  and  $0.700350 \pm 0.000075$ , respectively (Fig. 1) [9]. The scattering of initial  $^{87}\text{Sr}/^{86}\text{Sr}$  data around the weighted average of  $I_{\text{Sr}}$  (Fig.

1b) partially may be due to differing  $^{87}\text{Sr}/^{86}\text{Sr}$  in the target rocks.

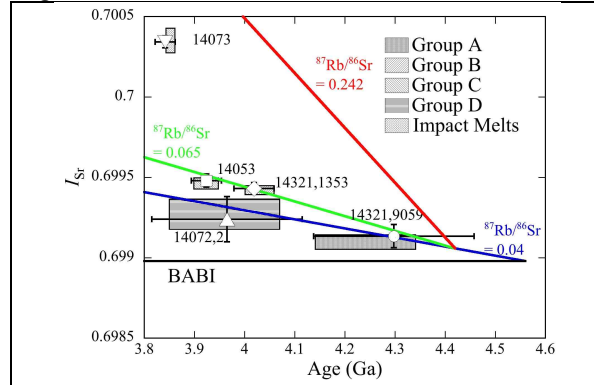


Fig. 2. Plot of weighted average of ages versus weighted average of initial  $^{87}\text{Sr}/^{86}\text{Sr}$  of each group. The red and blue lines are evolution paths of the bulk moon ( $^{87}\text{Rb}/^{86}\text{Sr} \approx 0.242$ ) and A14 KREEP ( $^{87}\text{Rb}/^{86}\text{Sr} \approx 0.04$ ) respectively. One sample in each group is also plotted.

**Geochemical Coherence within the High-Al Basalt Clan:** Using Rb-Sr isotopic provenance (Fig. 2) and ITE ratios [7,22], A-14 high-Al basalts can be classified into three groups (A, B and C) and a tentative fourth group (D). Group A and D basalts fall on the evolution path of the bulk moon [23,24] (blue line in Fig. 2), while Group B and C basalts fall between the evolution paths of the bulk moon [23,24] and A-14 KREEP [25,26]. This, coupled with distinct ITE ratios, indicates that Group B and C basalts were derived from at least two distinct source regions. When all A-14 high-Al basalts, regardless of the fact that they formed at different times (Fig. 1), are taken into consideration, a general hyperbolic mixing curve [27,28] can fit available whole-rock Rb-Sr isotopic data with two end members of Group A basalt and A-14 KREEP (average of 14161,35,2; 14161,35,4; 14307,26,1 and 14163,65,2) [25,26] (Fig. 3a). This implies that the parental melts of high-Al basalts underwent similar evolutionary histories but at different times [23].

The melt products and sources of the different high-Al basalt groups were examined using whole-rock ITE data [7]. Whole-rock ITE ratios of pristine A-14 high-Al basalts can also be modeled via mixing [27,28] with the two end members being the Group A basalt composition and urKREEP [26] (Fig. 3b). By examining the parental melts for each of the groups (derived by [7]), it would appear that each source region (excluding Group D due to lack of data) contained variable proportions of KREEP (inset to Fig 3b). This is in addition to the assimilation that these basalts experienced during crystallization [7,22,23]. This strengthens the conclusions that the parental melts of A-14 high-Al basalts are geochemically correlated and that a KREEP component was also present in the

Group B and C source regions, which is consistent with a previous study of olivine phenocrysts [29]. Both Rb-Sr isotopic compositions and ITE ratios show that parental melt compositions of A-14 high-Al basalts are genetically correlated through mixing of evolved components with a relatively primitive magma ocean cumulate.

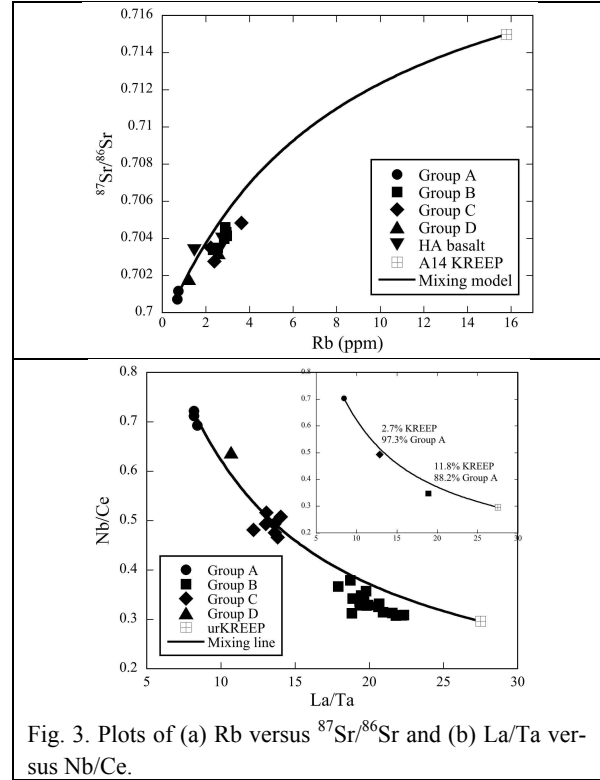


Fig. 3. Plots of (a) Rb versus  $^{87}\text{Sr}/^{86}\text{Sr}$  and (b) La/Ta versus Nb/Ce.

**References:** [1] Dasch et al. (1987) *GCA*, 51, 3241-3254.

- [2] Nyquist & Shih (1992) *GCA*, 56, 2213-2234. [3] Papanastassiou & Wasserburg (1971) *EPSL*, 12, 36-48. [4] Shearer et al. (2006) *RiMG*, 60, 365-518. [5] Dickinson et al. (1985) *LPS XV*, C365-C374. [6] Shervais et al. (1985) *LPS XV*, C375-C395. [7] Neal & Kramer (2006) *AM*, 91, 1521-1535. [8] Begemann et al. (2001) *GCA*, 65, 111-121. [9] Ludwig (2008) BGCS 4. [10] Neal et al. (2006) *LPS XXXVII*, #2003. [11] Compston et al. (1972) *LS III*, 1487-1501. [12] Mark et al. (1973) *LS IV*, 1785-1795. [13] Compston et al. (1971) *EPSL*, 12, 55-58. [14] Mark et al. (1975) *LS VI*, 1501-1507. [15] Mark et al. (1974) *LS V*, 1477-1485. [16] Dasch et al. (1991) *LPS XXII*, 275-276. [17] McKay et al. (1978) *LPS IX*, 661-687. [18] McKay et al. (1979) *LPS X*, 181-205. [19] Wasserburg & Papanastassiou (1971) *EPSL*, 13, 97-104. [20] Murthy et al. (1972) *LS III*, 1503-1514. [21] Tatsumoto et al. (1972) *LS III*, 1531-1555. [22] Hui et al. (2011) *GCA*, 75, 6439-6460. [23] Neal & Taylor (1990) *LPSC XX*, 101-108. [24] Nyquist (1977) *PCE*, 10, 103-142. [25] Nyquist et al. (1972) *LSC III*, 365-518. [26] Warren & Wasson (1979) *RGSP*, 17, 73-88. [27] Vollmer (1976) *GCA*, 40, 283-295. [28] Langmuir et al. (1978) *EPSL*, 37, 380-392. [29] Hagerty et al. (2005) *GCA*, 69, 5831-5845.